

Kinetics of Nickel and Vanadium Adsorption from Crude Oil onto NH_4Cl -modified Primitive Clay

Donald T. Kukwa^{*1,2}, Rose E. Ikyereve^{1,3}, Sylvester O. Adejo¹ and Chris O. Ikese¹

¹ Department of Chemistry, Benue State University, Makurdi – Nigeria

² Department of Chemical Engineering, University of Benin, Benin City – Nigeria

³ Department of Chemistry, Loughborough University, Loughborough, Leicestershire – United Kingdom

ABSTRACT

The kinetics of Ni and V adsorption from crude oil by NH_4Cl -modified primitive clay ($M_{\text{NH}_4\text{Cl}}$) was studied at 25°C and pH 4.8. The percentage removal of both metals was found to increase with increase in both adsorbent dosage and contact time. The data generated fitted the Lagergren's pseudo second-order kinetics model more than the Lagergren's pseudo first-order model. The adsorption process was found to be intra-particle diffusion-controlled, adopting the Weber and Morris model mainly within the first 720 min of the process. However, beyond 720 min of the Ni and V adsorption process onto $M_{\text{NH}_4\text{Cl}}$, surface adsorption mechanism prevailed. NH_4Cl -modified primitive clay is therefore competitive among low cost sorbents that can be used for Ni and V sequestration from crude oil.

KEYWORDS: NH_4Cl -modified Primitive clay, adsorption, pseudo second order kinetics, intra-particle diffusion.

Date of Submission: 29 July 2013



Date of Publication: 30 April 2014

I. INTRODUCTION

The unprecedented increase in the demand for petroleum products since the dawn of the 20th century [1] has made fluid catalytic cracking (FCC) a reaction of interest in the petroleum industry, as it is the sole process from which these products are obtained from crude oil [2]. However, the presence of catalyst deactivating metals such as Ni and V in crude oil has adverse effects on the economy of crude oil refining by the process of FCC. For example, vanadium poisons the catalyst used in FCC, while Ni causes coke deposition on it [3], thus resulting in reduced catalyst activity leading to astronomical costs in crude oil refining process. A few attempts have been made at removing these metals from crude oil by adsorption process [4, 5] prior to refining. Such attempts are either too complicated or failed totally to yield the desired product, quantitatively.

Clays have been reported to play important roles in the removal of cations and anions from the environment via adsorption and ion exchange processes. In our previous work [6], $M_{\text{NH}_4\text{Cl}}$ was found to give the highest removal efficiency of Ni and V from crude oil in comparison with several other modifications as well as with the unmodified clay. These, coupled with the fact that clays are readily available, easily prepared, stable in a wide range of conditions in comparison with other adsorbents and fall into the category of low cost adsorbent [7, 8] have informed their choice as sorbents for this study.

II. MATERIALS AND METHODS

Crude oil sample was obtained from the Port Harcourt Refinery, Port Harcourt, Rivers State- Nigeria, while the clay samples were collected from Makurdi, Benue State-Nigeria. The clay samples were beneficiated by the modified wet method [9]. 100g of the beneficiated clay was treated with 150mL of 1M NH_4Cl in a 250mL conical flask and the slurry equilibrated for 24 h and then air-dried for 96 h and ground to fine powder in a porcelain mortar to obtain the $M_{\text{NH}_4\text{Cl}}$.

The initial concentrations, C_o (mg/L), of Ni and V in the untreated crude oil were determined using a Shimadzu atomic absorption spectrophotometer model AA 6800 [10]. Mineral composition of the clay sample was determined by a thermo 9900 intellipower X-ray fluorescence spectrophotometer [11]. The physicochemical properties determined for the primitive clay were bulk density, moisture content, pH, porosity and cation exchange capacity [6].

The adsorption experiment was conducted in batch mode. 50mL each of crude oil samples contained in separate 250mL conical flasks were separately treated with graded amounts of M_{NH_4Cl} (0.1g, 0.2g, 0.3g, 0.4g, 0.5 g, 0.6g, 0.7g, and 0.8g) and agitated using an electrical shaker 360rpm for 600 min and then allowed to equilibrate for 1320min at 25°C . The content of each flask was then centrifuged at 6000rpm and the supernatant oil decanted. 10mL portion of each supernatant was measured separately into a porcelain crucible and ashed in a muffle furnace at 800°C for 240min. The ash was then digested with 4mL concentrated HCl and made up to 50mL in a 50mL volumetric flask after quantitative rinsing. The concentrations of Nickel and Vanadium C_t (mg/L) remaining in the clay-treated oil at time t (min) as well as at equilibrium C_e were determined using AAS. The percentage adsorption was then evaluated using equation (1).

$$\text{Percentage Adsorption (\%)} = \frac{C_o - C_e}{C_o} \times 100 \quad (1)$$

where C_o and C_e (mg/L) are the metal concentrations in the sample before treatment and at equilibrium. The adsorption capacity at equilibrium q_e (mg g⁻¹) is determined using equation (2).

$$q_e = (C_o - C_e) \times \frac{V}{M} \quad (2)$$

where V is the volume (L) of treated sample, M is the mass (g) of adsorbent added.

The effect of contact time on percentage adsorption, can be monitored when the dosage of the adsorbent is fixed (in our case 0.5 g) while varying the contact time. The percentage adsorption for each time interval was calculated as earlier described. The adsorption capacity at various time intervals q_t (mg g⁻¹) was determined using equation (3).

$$q_t = (C_o - C_t) \times \frac{V}{M} \quad (3)$$

III. ADSORPTION KINETICS MODELS

The importance of kinetics studies in adsorption is due to the fact that the mechanism of the adsorption process can be understood from the kinetics constants. The rate of adsorption that controls the resistance time can also be determined [12]. Many theories and models have been conceptualized to describe the kinetics of the equilibrium distribution of a solute between the dissolved (liquid) and adsorbed (solid) phases for adsorption process [9]. These models are of different shapes depending on the type of adsorbent, adsorbate and intermolecular interactions between them. Three of such models tested in the present study are the pseudo first- and second-order models and the intra-particle diffusion models.

The pseudo first-order model

The Lagergren's pseudo first-order and pseudo second-order kinetic equations are used to model the adsorption processes [13, 14, 15].

The Lagergren's pseudo first-order expression is given by equation (4).

$$\frac{dq_t}{dt} = k_1(q_e - q_t) \quad (4)$$

where q_e and q_t (mgg⁻¹) are the adsorption capacities of the adsorbent at equilibrium and at time t respectively. k_1 (min⁻¹) is the Lagergren's pseudo first-order rate constant for the adsorption process and t the contact time in minutes. The integrated rate law after applying the initial conditions of $q_t = 0$ at t = 0 gives equation (5)

$$\log(q_e - q_t) = \log q_e - \frac{k_1}{2.303} \cdot t \quad (5)$$

k_1 is obtained from the slope of a plot of $\log(q_e - q_t)$ against t.

The pseudo second-order model

The pseudo second-order rate equation [10] is given in equation (6).

$$\frac{dq_t}{dt} = k_2(q_e - q_t)^2 \quad (6)$$

where k_2 is the pseudo second-order rate constant for the adsorption process (mgg⁻¹min⁻¹).

On integration of equation (6) from t=0 to t=t and $q_t = 0$ to $q_t = q_t$, equation (7) is obtained.

$$\frac{t}{q_t} = \frac{1}{k_2 q_e^2} + \frac{1}{q_e} \cdot t \quad (7)$$

The initial adsorption rate, h ($\text{mg g}^{-1} \text{min}^{-1}$) [15] is given in equation (8).

$$h = k_2 q_e^2 \quad (8)$$

Then, equation (7) becomes

$$\frac{t}{q_t} = \frac{1}{h} + \frac{1}{q_e} \cdot t \quad (9)$$

The plots of $\frac{t}{q_t}$ against t give a straight line with intercept at $\frac{1}{h}$ from which can be evaluated, and hence k_2 .

Intra-particle diffusion models

The intra-particle diffusion model suggested by McKay and Poots [11, 12] is expressed in equation (10).

$$q_t = k_p t^{1/2} + C \quad (10)$$

where t is time (min) and k_p ($\text{mg g}^{-1} \text{min}^{-1/2}$) is the intra-particle diffusion rate constant. k_p is obtained from the slope of a plot of q_t versus \sqrt{t} .

Weber and Morris [16] suggested another intra-particle diffusion model, which is given in equation (11) and which was been tested by different researchers [17, 18]

$$R = \ln k_{id} + n \ln(t) \quad (11)$$

Where R is the percent metal adsorbed; k_{id} is the inter-particle diffusion rate constant, which is a rate factor (min^{-1}); n is the slope of the linear plots, which describes the adsorption mechanism; and t is the contact time.

IV. RESULTS AND DISCUSSION EFFECT OF ADSORBENT DOSAGE ON PERCENT ADSORPTION OF NI AND V

Figure 1 show that the percentage adsorption of Ni increased progressively and almost linearly with increase in adsorbent dosage from 0.1 to 0.6 g while that of V increased progressively as the adsorbent dose increased from 0.1 to 0.7 g. The progressive increment in metal ion adsorption could be due to increased availability of adsorption sites on the adsorbent [8]. Maximum removal values of 97.6% and 98.6% were attained at the dosage of 0.8 g of the sorbent for Ni and V respectively. Adsorbent dosages between 0.6 and 0.8 g gave exponential removal of metal ions [19, 20], which may be due to poor agitation leading to inadequate exposure of adsorptive surface [8]. The optimum adsorbent dose for Ni and V adsorption with $\text{M}_{\text{NH}_4\text{Cl}}$ fell between 0.7 and 0.8 g of clay per 50 mL of crude oil.

V. EFFECT OF CONTACT TIME ON PERCENT ADSORPTION OF Ni AND V

Figure 2 shows that the percentage adsorption of Ni and V on $\text{M}_{\text{NH}_4\text{Cl}}$ increases progressively with increase in contact time and attains a maximum as from 720 minutes for Ni and 840 minutes for V. Thereafter, no significant increase in adsorption occurred which may likely be due to saturation of the adsorption sites on the adsorbent [21]. The percentage removal of Ni is marginally higher than that of V as depicted by the figure. The faster removal rate at the initial time may be due to the availability of uncovered surface area of the adsorbent [22].

VI. ADSORPTION KINETICS STUDIES

Lagergren models

The pseudo first-order plot for Ni adsorption (Figure 3) gives a straight line with a regression coefficient (r^2) of 0.9984. The pseudo first-order rate constant (k_1) evaluated from the slope was $4.6 \times 10^{-3} \text{ min}^{-1}$. The equilibrium adsorption capacity (q_e) of 0.01 mg g^{-1} was obtained. However, this value does not correspond with the experimental value obtained in Table 4, hence the need for a pseudo second-order adaptation. The pseudo first-order plot for V adsorption (Figure 4) gives a straight line with a regression coefficient of 0.853. The pseudo first-order rate constant (k_1) calculated from the slope was $-4.6 \times 10^{-3} \text{ min}^{-1}$ and the equilibrium adsorption capacity (q_e) calculated from the intercept is 0.081 mg g^{-1} . Also, this value does not correspond with the experimental value obtained in Table 5 hence the need for a pseudo second-order adaptation.

The pseudo second-order plot for the Ni adsorption (Figure 5) gives a straight line with regression coefficient of 0.9934. The pseudo second-order rate constant (k_2) calculated from the intercept is $4.28 \times 10^0 \text{ g mg}^{-1} \text{min}^{-1}$ and the equilibrium adsorption capacity (q_e) calculated from the slope is 0.02 mg g^{-1} . However this value corresponds more closely with the experimental value obtained in Table 4. Therefore, the adsorption of Ni onto $\text{M}_{\text{NH}_4\text{Cl}}$ fit better into Lagergren's pseudo second-order kinetics. This result is in good agreement with other works [8, 12, 13, 17, 18, 20] and it means that the rate-determining step could be the chemical interaction between adsorbent sites and metal ions [8]. The pseudo second-order plot of V adsorption (Figure 6) gives a straight line with regression coefficient of 0.9943. The pseudo second-order rate constant (k_2) calculated from the intercept is $5.84 \times 10^{-2} \text{ g mg}^{-1} \text{min}^{-1}$ and the equilibrium adsorption capacity (q_e) calculated from the slope is 0.169 mg g^{-1} . This value corresponds more closely with the experimental value of 0.152 mg g^{-1} obtained in Table 5. Therefore, the adsorption of V onto $\text{M}_{\text{NH}_4\text{Cl}}$ best fitted into Lagergren's pseudo second-order kinetics. The same observation made above also holds for this metal.

Intra-particle Diffusion

The intra-particle diffusion McKay and Poots plots [18] for Ni and V adsorptions are as shown in Figures 7 and 8 respectively. Both plots of q_t versus \sqrt{t} for the Ni and V adsorption on $\text{M}_{\text{NH}_4\text{Cl}}$ gave straight lines at the start but after a while, a parabolic curve ensued signifying deviation from linearity due to clogging of surface pores and posing serious competition for the available ones. However, both do not pass through the origin, an indication that, although the metal sorption is intra-particle diffusion-controlled at the start, it is not the sole rate limiting step for the adsorption process on $\text{M}_{\text{NH}_4\text{Cl}}$ [19]. The value of regression coefficient for Ni adsorption (0.8043) is higher than that for V (0.7687), showing that data from Ni adsorption fitted better into the McKay and Poots model compared with V.

The values of k_p obtained from the slopes of the Ni and V adsorption in these plots are 0.0004 and $0.0032 \text{ mg g}^{-1} \text{ min}^{-0.5}$ respectively. The higher the k_p value, the higher would be the rate of metal adsorption. However similar studies [8, 17] have shown that k_p increases with increase in the initial concentration of the adsorbate in the sample matrix. The intercept C obtained for the Ni and V adsorptions (Figures 7 and 8) are 0.0086 mg g^{-1} and 0.0641 mg g^{-1} respectively. These values represent the thickness of the boundary layer. The larger these values, the greater would be the contribution of surface adsorption in the rate controlling step.

The Weber and Morris intra-particle diffusion plots [16, 18] gave the Ni regression equation as expressed in equation (12) with a regression coefficient of 0.8513; the V regression equation is expressed in equation (13) with a regression coefficient of 0.8335.

$$y = 14.325x - 19.216 \quad (12)$$

$$y = 13.92x - 21.179 \quad (13)$$

Thus, the intra-particle diffusion rate constant, k_{id} , for Ni and V are respectively $4.5144 \times 10^{-9} \text{ min}^{-1}$ and $6.3398 \times 10^{-10} \text{ min}^{-1}$. These are relatively low rates compared with the McKay and Poots model; but the high regression coefficient values of the Weber and Morris model signifies that it is a superior model to adopt for both Ni and V adsorption onto $\text{M}_{\text{NH}_4\text{Cl}}$.

VII. CONCLUSION

Percent adsorption of Ni and V on $\text{M}_{\text{NH}_4\text{Cl}}$ increases with increase in adsorbent dosage with the optimum adsorbent dose between 0.7 and 0.8 g per 50 mL of crude oil. The percent adsorptions of both metals were also found to increase with increase in contact time but attained a maximum at 600min for Ni and 840min for V. The adsorption of Ni and V onto $\text{M}_{\text{NH}_4\text{Cl}}$ is best described by Lagergren's pseudo second-order kinetics; and was found to be intra-particle diffusion-controlled, adopting the Weber and Morris model mainly within the first 720 min of the process. However, beyond 720 min of the Ni and V adsorption process onto $\text{M}_{\text{NH}_4\text{Cl}}$, surface adsorption mechanism prevailed. NH_4Cl -modified primitive clay is therefore competitive among low cost sorbents that can be used for Ni and V sequestration from crude oil.

VIII. ACKNOWLEDGEMENTS

The authors are grateful to KRPC Kaduna and NNPC Port Harcourt, Nigeria for the supply of crude oil samples. The Chemistry Departments of both, the University of Loughborough, Loughborough, Leicestershire, United Kingdom and Benue State University, Makurdi, Benue State, Nigeria are very highly appreciated.

REFERENCES

- [1] Philip, M. (2003). Advanced Chemistry, 1st edition, New Delhi Foundation Books, pp. 525-526.
- [2] Reynolds, J. G. (2004). Removal of Ni and V from heavy crude oils by exchange reactions. *Am.chem.soc.* 49(1):79.
- [3] Conghua, L., Youquan, D., Yuanqing, P., Shygin, Z., and Xionghou, G. (2004). Interactions between heavy metals and clay matrix in fluid catalytic cracking catalysts. *Applied catalysis* 257:145-147.
- [4] Cha, C.Y., Boysen, J.E. and Branthaver, J.F. (1991). Process for removing heavy metal compounds from heavy crude oil, US patent: 5041209 to Western Research Institute Laraimie.
- [5] Brannvall, E.G., Mazeikiene, A. and Valentukeviciene, M. (2006). Experimental research on sorption of petroleum products from water by natural clinoptilolite and vermiculite. *Geological.* 5: 5-12.
- [6] Kukwa, D. T., Ikereye, R. E., Adejo, S. O. and Ikese, C.O. (2013). Characterization of primitive clays from Katsina-Ala and Makurdi, Benue State-Nigeria. *Journal of Chemistry and Materials Research* (In print)
- [7] Medvedeva, M.L. (2002). Specifics of high-temperature corrosion processes during oil recovery. *Chemical and Petroleum Engineering.* 36: 11-12.
- [8] Wambu, E. W., Muthakia, G. K., wa-Thiog'o, J. K. and Shiundu, P. M. (2011) Kinetics and thermodynamics of aqueous Cu (II) adsorption on heat regenerated spent bleaching earth. *Bulletin of Chemical Society of Ethiopia.* 25(2): 181-190
- [9] Yakout, S. M. and Elsherif, E. (2010). Batch Kinetics, isotherm and thermodynamic studies of adsorption of strontium from aqueous solutions onto low cost rice straw based carbon. *Applied science innovations Pvt. India carbon-Sci. Tech.* 149p

- [10] Acevedo, S., Ranaudo, M.A., Fernandez, Z.A., Castillo, J. and Garcia, C. (2003). Energy. Fuels. 17: 257.
- [11] Masooleh, M. S., Bazgir, S., Tamizifar, M. and Nemati, A. (2010). Adsorption of petroleum hydrocarbon on organoclay. Journal of Applied Chemical Research, 4(14): 19-23.
- [12] Radnia, H., Ghoreyshi, A. A. and Younesi, H. (2011) Isotherm and Kinetics of Fe(II) adsorption onto chitosan in a batch process. Iranica Journal of Energy and Environment 2(3), 250-257
- [13] Kara, M., Yuzer, H., Sabah, E. and Celik, M. S. (2003). Adsorption of cobalt from aqueous solutions onto sepiolite. Water Res. 37: 948.
- [14] Bhattacharyya, K.G. and Sengupta, S. (2006). Pb^{2+} uptake by kaolinite and montmorillonite in aqueous medium: influence of acid activation of the clays. Colloid Surf. A: physicochem. Eng. Aspects. 277: 191
- [15] Demirbas, E., Koby, M., Senturk, E. and Ozkan, T. (2004) Adsorption kinetics for the removal of chromium (VI) from aqueous solutions on the activated carbons prepared from agricultural wastes. Water SA 30(4): 533-539
- [16] Weber, W. J. and Morris, J. C. (1963). Kinetics of adsorption on carbon from solution. J. Sanit Eng. Div. ASCE, 89: 31-59
- [17] Srivastava, S. K., Tyagi, R. and Pant, N. (1989). Adsorption of heavy metal ions on carbonaceous material developed from the waste slurry generated in local fertilizer plants. Water Res., 23: 1161-1165
- [18] Odoemelam, S. A., Iroh, C. U., and Igwe, J. C. (2011). Copper (II), Cadmium (II) and Lead (II) Adsorption kinetics from aqueous metal solutions using chemically modified and unmodified cocoa pod husk (*Theobroma cacao*) waste biomass. Res. J. Appl. Sc. 6(1): 44-52
- [19] Yakout, S.M. and Elsherif, E. (2010). Batch kinetics, isotherm and thermodynamic studies of adsorption of strontium from aqueous solutions onto low cost rice-straw based carbon. Applied science innovations Pvt. India carbon-Sci. TechPp 149.
- [20] Renugadevi, N., Sangeetha, R., and Lalitha, P. (2011). Kinetics of the adsorption of methylene blue from an industrial dyeing effluent onto activated carbon prepared from the fruits of *Mimusops elengi*. Archives of Applied Science Research. 3(3):494.
- [21] Balabin, R. M., and Syuyayev R. Z. (2008). Petroleum resins adsorption onto quartz sand: Near infrared (NIR) spectroscopy study. Journal of colloid and interface Science 3(8):167.
- [22] Abia, A. A. and Asuquo, E. D. (2006). Lead (II) and Nickel (II) adsorption kinetics from aqueous metal solutions using chemically modified and unmodified agricultural adsorbents. African Journal of Biotechnology 5(16): 1475-1482

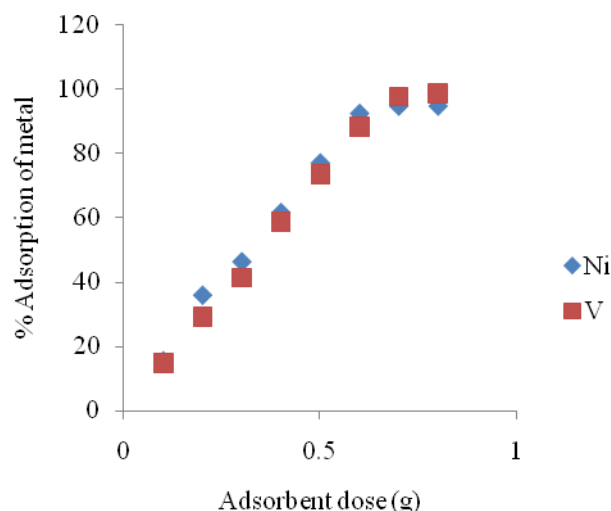


Figure 1 Variation of percent Ni and V adsorption with adsorbent dose

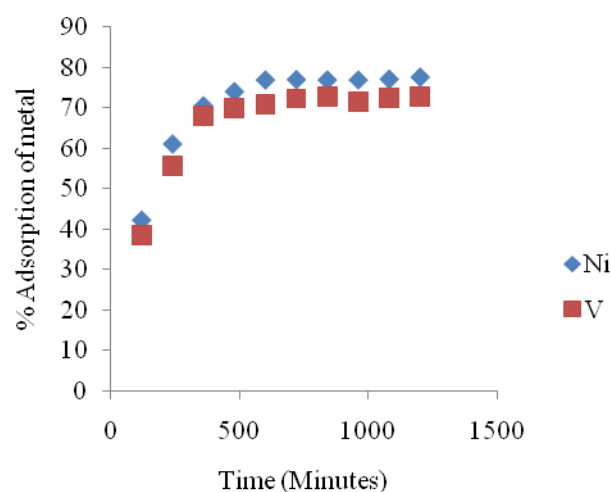


Figure 2 Variation of percent Ni and V adsorption with contact time

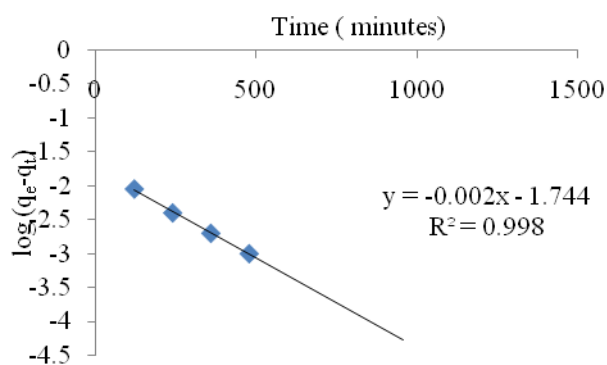


Figure 3 Pseudo first-order kinetic plots for Ni adsorption

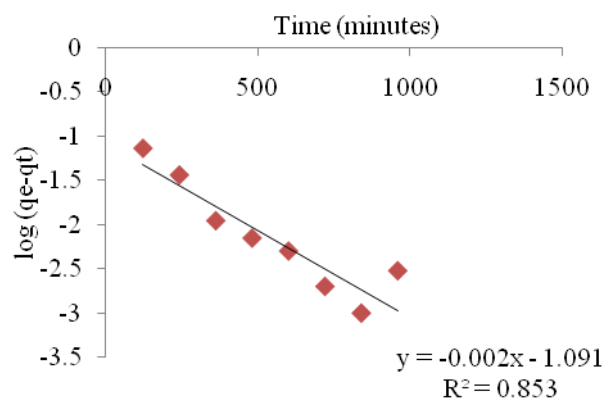


Figure 4 Pseudo first order kinetics plots for V Adsorption

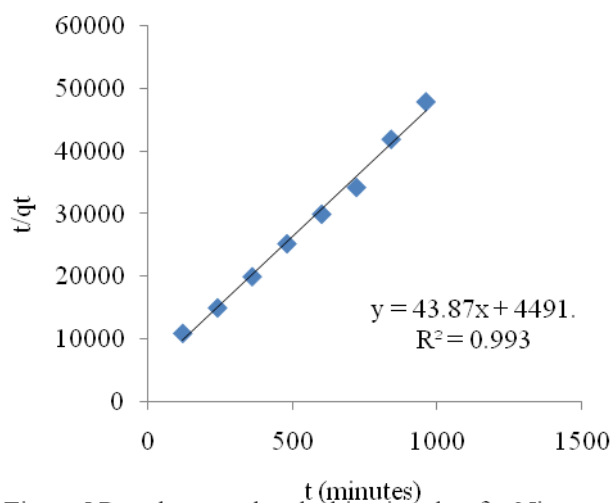


Figure 5 Pseudo second-order kinetics plots for Ni adsorption

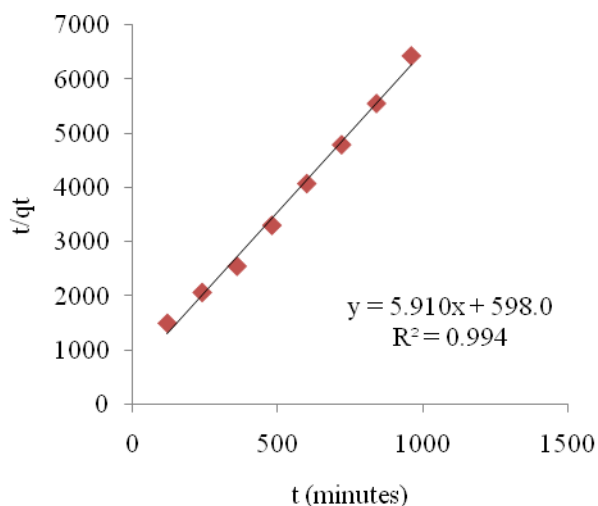


Figure 6 Pseudo second-order kinetics plots for V adsorption

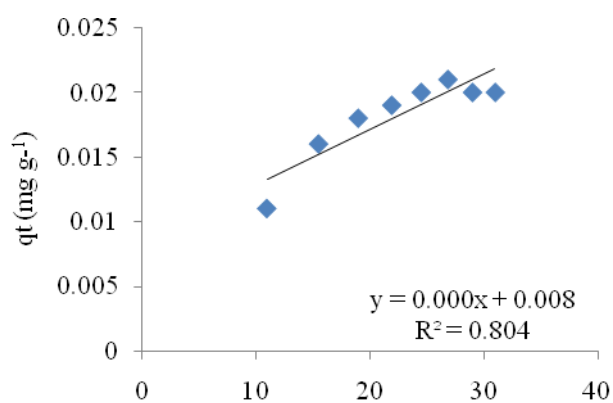


Figure 7 Intra-particle diffusion plots for Ni adsorption

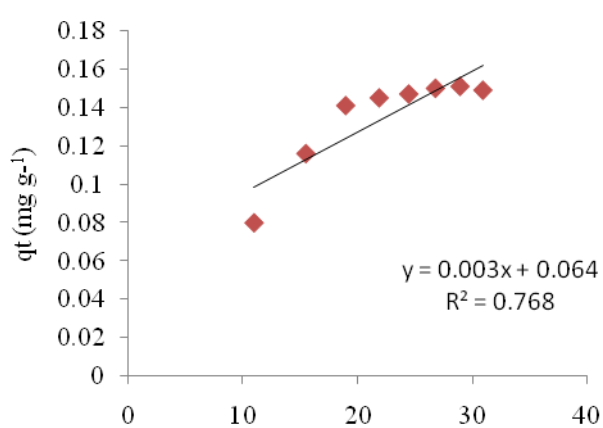


Figure 8 Intra-particle diffusion plots for V adsorption

Table 1 Metal composition of untreated crude oil

Metal	Ni	V	Fe	Na	K	Pt	Pd
Concentration C _o (mg L ⁻¹)	0.26	2.07	0.81	16.42	0.09	0.53	9.21

Table 2 Percent mineral composition of beneficiated and unbeneficiated clay samples

Clay sample	SiO ₂	Al ₂ O ₃	Fe ₂ O ₃	CaO	MgO	Na ₂ O	K ₂ O
Unbeneficiated	82.64	13.86	4.79	0.99	0.71	0.07	2.44
Beneficiated	78.94	13.68	4.68	2.32	0.77	0.01	2.42

Table 3 Physicochemical Properties of Clay Sample collected from Makurdi

Bulk density (g/cm ³)	Moisture content (%)	pH	porosity	CEC (meq/100g)
1.8	17.65	4.8	0.32	3.1

Table 4 Percent and equilibrium Ni adsorption capacity of clay samples

Type of clay modification	Average	Percent adsorption (%)	Equilibrium
	Equilibrium		adsorption
	Concentration		capacity, q _e
	of Ni in oil, C _e (mgL ⁻¹)		(mgg ⁻¹)
M _{un}	0.19 ± 0.02	27.9	0.007
M _{HCl}	0.11 ± 0.02	58.7	0.015
M _{H₂SO₄}	0.09 ± 0.06	65.4	0.017
M _{H₃PO₄}	0.08 ± 0.02	69.2	0.018
M _{NH₄Cl}	0.06 ± 0.03	77.9	0.020

Table 5 Percent and equilibrium V adsorption capacity of clay samples

Type of clay Modification	Average	Percent adsorption (%)	Equilibrium
	Equilibrium		adsorption
	Concentration		capacity, q _e
	of V in oil, C _e (mgL ⁻¹)		(mg/g)
M _{un}	1.98 ± 0.06	4.34	0.009
M _{HCl}	1.07 ± 0.08	48.30	0.100
M _{H₂SO₄}	0.99 ± 0.08	52.17	0.108
M _{H₃PO₄}	0.61 ± 0.01	70.53	0.146
M _{NH₄Cl}	0.55 ± 0.10	73.43	0.152